

Development of a Method for CFD Evaluation of Helicopter Fuselages

R. Heise, C.J. Meyer, T.W. von Backström
 Department of Mechanical Engineering
 University of Stellenbosch
 South Africa

Abstract

This paper presents the findings of simulating a helicopter fuselage in the presence of a rotor, using computational fluid dynamics. The objective is to simulate steady state rotorcraft fuselage aerodynamics with the intention of forming a basis by which finer points of rotorcraft aerodynamics can be simulated, such as the performance of intakes fitted to the vehicle. An actuator disc rotor model is used for the current simulations as this saves computing resources by not having to model individual blades with moving grids. The analysis presented here was conducted on the ROBIN fuselage, as substantial experimental data is available on this configuration. Initially a trial series was conducted on a fuselage-only configuration. This served to develop confidence in the mesh and turbulence models eventually used on the full rotor and fuselage simulations. Good agreement was obtained with the experimental data. The fuselage and rotor combination was modelled as being mounted in a 14- by 22- foot wind tunnel as in the experiments. The actuator disc model used for the simulations is unique in that it calculates the section angle of attack by referencing to upstream and downstream values of the rotor disk, unlike standard models which reference to the flow inside the disc. Thus more accurate answers can be obtained, even for skewed inflows. Acceptable results were obtained here, with the asymmetric pressure distribution being captured, though noticeable differences are detected. The rotor hub was also included in the simulations, also modelled as an actuator disk.

Notation

A_1, B_1	Cyclic pitch angles [degrees]
C_p	Pressure coefficient, $C_p = \frac{P}{\rho V_t^2} \times 100$
C_T	Thrust coefficient, $C_T = \frac{T}{\rho \pi R^2 V_t^2}$
R	Rotor radius, also forms parameter for ROBIN fuselage [m]
U	Freestream velocity [m/s]
V_t	Rotor tip velocity [m/s]

α_s	Rotor shaft angle [degrees]
ϕ	Polar angular coordinate used for the definition of the ROBIN fuselage [degrees]
μ	Advance ratio, $\mu = \frac{U}{V_t}$
Ω	Rotor speed, 2000rad/s
θ_o	Rotor collective pitch angle [degrees]
ρ	Air density [kg/m ³]
σ	Rotor solidity
ψ	Rotor azimuth angle [degrees]

Actuator Disk

Much development has been done on actuator disks for applications in helicopters, either for rotor performance analysis or fuselage aerodynamics, with various degrees of successes having been achieved (Chaffin et al⁽¹⁾, Lee et al⁽²⁾). Recently computing resources became available that allow for detailed and transient analyses of helicopter aerodynamics. For helicopter fuselage aerodynamic evaluations an actuator disc model is sufficient if a non-transient solution is sought that requires the modelling of the passage of the blades and associated tip vortices. The current study investigates the agreement of the numerical solutions with experimental data, to form a basis for further aerodynamic studies, such as intake performance.

A new approach to the modelling of the actuator disk is used. Air approaching an airfoil experiences an up wash ahead of the airfoil, and thus the section angle of attack must be measured upstream of the airfoil section. Thus for an actuator disk the section angle of attack must be picked up a small distance upstream of the of the actuator disk, as first suggested by Thiant⁽³⁾ and refined by Meyer et al⁽⁴⁾. The section angle of attack is calculated by the flow values a finite distance ahead of the of the actual actuator disk and behind it. This concept has been shown to give exceptional results when compared to the experimental data of skew inflows to industrial fans (Hotchkiss⁽⁵⁾). These results gave confidence to use the same code to model helicopter rotors.

The actuator disk forms a volume in the flow domain that is normally occupied by the rotor into which the momentum sources are introduced, with an identically meshed volume upstream and downstream of the rotor volume. The upstream volume is placed about one blade chord length directly above the actuator disk (though not perfectly upstream), with a sufficiently fine mesh in between to capture the spin-up of the incoming flow. The error of the blade section angle of attack formed by placing the upstream disk not strictly upstream is assumed to be small, at least at slow advance ratios, flow vectors do not change significantly for a given small region that affects a given blade section. This could however be a problem at high advance ratios. The actuator disk for the current application does not include any coning or tilt of the tip path plane, but blade pitching was modelled using the standard Fourier harmonic series of

$$\theta = \theta_0 - A_1 \cos \psi - B_1 \sin \psi \quad 1$$

Balancing of the rotor was done on an iterative basis, with the assumption that the response to the pitching coefficients is linear.

Fuselage Only Simulations

In preparation the ROBIN fuselage was evaluated without the rotor to define mesh sizing and compare turbulence models. Experimental data based on the work by Freeman et al⁽¹⁾ is available of a ROBIN fuselage only configuration in a wind tunnel. For this test case the fuselage was modelled at an angle of attack of -10° with zero yaw. Due to the symmetry only one half of the flow domain was simulated. The experimental data is however not exactly symmetrical. The experimental data is in the form of pressure measurements taken at several stations on the fuselage surface, which are compared to the CFD data.

The near wall mesh was constructed to give y^+ values of below $y^+ = 4$ for the expected flows around the fuselage. An y^+ value of 4 or less was selected that the laminar sub layer would be resolved for better results from the turbulence models. A guess for the height of the first element can readily be determined from basic boundary layer theory along with the thickness of the boundary layer itself. It was further aimed to keep at least 10 elements in the estimated boundary layer for sufficient resolution of the entire boundary layer. The mesh near the wall consisted of prismatic elements, and for this specific application of the 2 metre ROBIN fuselage the first element had a height of 0.05mm. After reducing the surface mesh to 15mm (0.75% of fuselage length) grid independence was obtained. This is of

the same order as the mesh used by Chaffin et al⁽¹⁾ for similar studies. Full use was made of the unstructured mesh to allow the elements to grow to the selected volume mesh size. Four volume mesh sizes here used and tested for grid convergence; namely 35, 30, 25 and 20 mm. For all sizes good agreement to the experimental data was obtained, with the change from 25 to 20mm not yielding any significant improvements. The coarser 35mm mesh is still useful as sufficiently accurate answers are still obtained and fewer computing resources are required.

Consecutive tests were done on all the grid sizes to select a turbulence model. Turbulence Models that were evaluated were the $k-\epsilon$, $k-\omega$, Shear Stress Transport (SST), Spalart-Allmaras and Detached Eddy Simulation (DES) models. Surface pressures were compared along four cross-sectional stations as indicated in Figure 1 to Figure 4. The data presented here is for the 25mm volume and 15mm surface mesh. The pressures are non-dimensionalised with the wind tunnel free stream conditions, which for this case is 21.2m/s at standard atmospheric conditions.

The data on the cross sectional stations is presented as a function of ϕ , the polar angular coordinate used for the definition of the ROBIN fuselage. The use of ϕ instead of the commonly used z coordinate allows for a better presentation and comparison of the data on the upper and lower surfaces of the fuselage.

Good agreement with the experimental data is obtained for all the models over most of the cross sections. At the first station at $x = 0.350R$ (Figure 1) the $k-\omega$ model gives an unrealistically high pressure on the upper surface ($\phi = 90^\circ$) along with a too low pressure below the fuselage. At the station just behind the cowling (Figure 2) most turbulence models give good answers, with the SST and $k-\omega$ models lying closest to the experimental data. The Spalart-Allmaras and DES models give almost identical results, which results from the near wall treatment of the DES model with the Spalart-Allmaras model and the fact that no significant flow separation occurs to modify the global flow pattern. All models however under-predict the pressure on top of the fuselage ($\phi = 90^\circ$), which could be as a result of the over-prediction of the wake of the cowling. The difference between experimental and numerical data at the bottom of the fuselage is as a result of the wake of the model support strut, which is not modelled in the CFD simulations. The last two stations at $x = 1.135R$ and $x = 1.540R$ (Figure 3 and Figure 4) show a separation point on the side of the fuselage at around the $\phi = 60^\circ$ radial, which can be seen by the sharp reversal of the pressure plot. None of the evaluated turbulence models

captured the separation point exactly, with the SST model coming closest. The $k-\omega$ model however predicts the pressure distribution on the bottom half the best. The discrepancy between the numerical and experimental data at the last two cross sections is assumed to be, in part, due to an insufficiently fine surface mesh that will capture the separation point correctly.

For the range of turbulence models tested, on average, the SST model performs the best over the range of compared experimental data. It is thus the model selected to be used for the full rotor and fuselage simulations. These CFD simulations were conducted using Fluent 6.1. Subsequent test runs with the later release, version 6.2, yielded better answers than the older results, the 35mm mesh giving more accurate results than the 20mm mesh on the 6.1 solver. This follows as a result of the improved numerics in the solver for better spatial accuracy, especially for tetrahedral meshes such as used for the current application (Fluent News⁽⁶⁾). For consistency only the results of the 6.1 solver are shown.

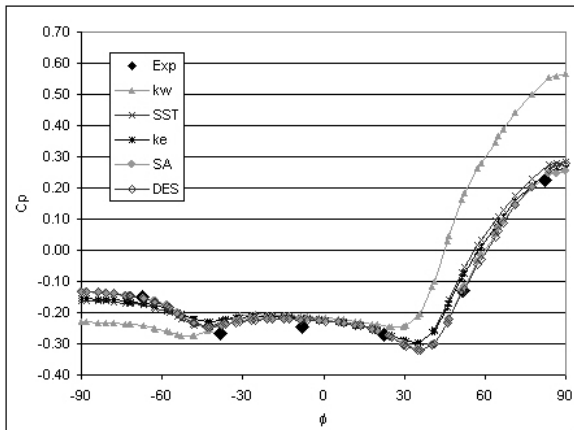


Figure 1 Pressure Distribution, Fuselage only, $x = 0.350R$

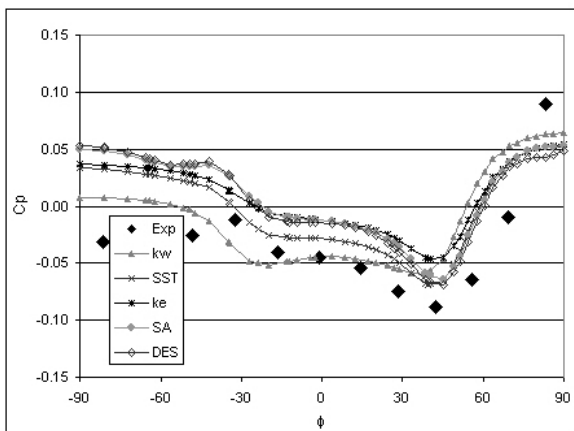


Figure 2 Pressure Distribution, Fuselage only, $x = 1.170R$

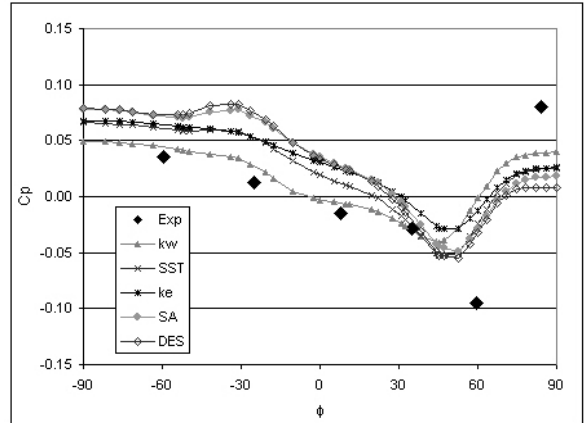


Figure 3 Pressure Distribution, Fuselage only, $x = 1.350R$

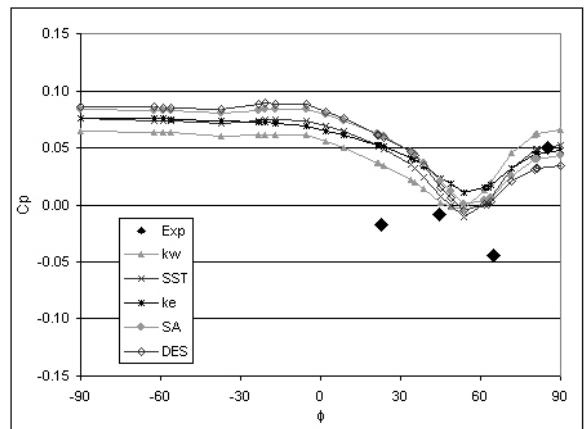


Figure 4 Pressure Distribution, Fuselage only, $x = 1.540R$

Rotor and Fuselage Simulations

For the initial validation process presented here of using the actuator disk as a helicopter rotor, the simulation was done for one advance ratio and thrust coefficient only. A case from Mineck et al⁽⁷⁾ was selected with an advance ratio of $\mu = 0.05$ and a thrust coefficient of $C_T = 0.00636$. A low advance ratio case was chosen as in such a case the rotor wake impinges on most of the fuselage and the inflow into the rotor is sufficiently skewed to test the capabilities of the actuator disk as a helicopter rotor. The rotor and fuselage combination was again modelled as being in the 14 by 22ft wind tunnel. The mesh was based on the results of the previous fuselage only trials, this time however the entire flow domain was included to capture the 3D flow effects from the rotor. Added to the actuator disk model that simulates the rotor blades, was a second actuator disk (volume) that modelled the rotor hub, as shown in Figure 5. Here the section lift and drag properties for the hub were defined as those of a cylinder. It is thought that the presence of the rotor hub can have a noticeable effect on the aerodynamics of the fuselage, especially in the region of the cowling.

Two sets of experimental data are available for the selected test case, namely from Mineck and Freeman et al⁽⁶⁾. The CFD model was defined to mimic the Mineck tests. The difference of the Mineck data is that a smaller rotor of 0.86 times the defined rotor radius for the ROBIN geometry is used with a solidity of $\sigma = 0.098$ compared to the solidity of $\sigma = 0.0871$ of the Freeman data. However both data sets are used for comparison as they show the same trends of the pressure distribution.

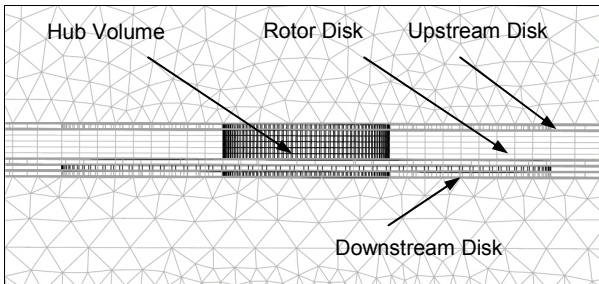
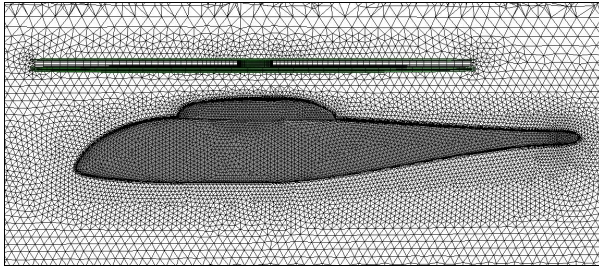


Figure 5 Mesh Configuration for ROBIN and Detail of Rotor and Hub Mesh

Qualitative analysis

When qualitatively comparing the CFD data to the oil flow experiments done by Mineck et al⁽⁷⁾ one notices that the streak lines for the selected thrust coefficient of $C_T = 0.00636$ do not follow the experimental streak lines closely. The angle of the numerical streak lines is too shallow, almost suggesting that the thrust coefficient used is too low. Based on this assumption a run was conducted for twice the specified thrust coefficient, and for this case the streak lines compare better with the experiments.

Figure 6 graphically compares the two cases to the experimental results on the advancing side of the fuselage; the dark streak lines are from the numerical simulations. On the nose and centre sections the streak lines are better predicted by the high thrust case. The streak lines on the cowling are also better captured with the high thrust case, as well as the wake of the hub at the trailing edge of the cowling and the convection of this wake down the starboard side that is evident from the experiments. None of this is seen in the standard case, the streak lines again only conforming rearwards of the cowling.

On the retreating side shown in Figure 7 the nose forward of the rotor wake the streak lines predicted by the double thrust case are again much better predicted, similar also in the mid-fuselage section. The influence of the hub-wake, which is evident in the experiments, is also only presented in the high thrust case. Only towards the rear of the fuselage behind the cowling do the original results again compare well with the experiments. On the cowling the streak lines are not well presented.

Quantitative Analysis

The rotor was iteratively balanced to have a zero moment around the hub. Table 1 shows the collective and pitch angles obtained for the two cases, along with the experimental values from Mineck et al⁽⁷⁾. The difference between the experimental and numeric values for the $C_T = 0.00636$ conditions can mainly be attributed to a lack of coning of the rotor actuator disk.

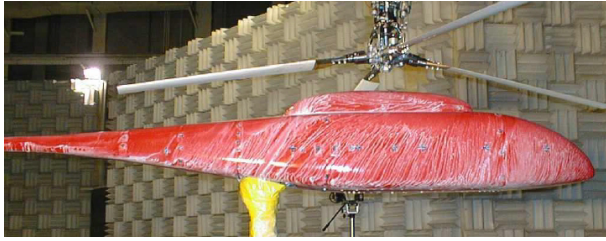
Table 1 Trimmed pitch conditions

Case	θ_o	A_1	B_1	α_s
Mineck et al ⁽⁷⁾ , $C_T = 0.00636$	11.9°	-1.3°	1.3°	0.0°
CFD, $C_T = 0.00687$	8.35°	-2.11°	1.25°	0.0°
CFD, $C_T = 0.0134$	14.72°	-1.73°	2.70°	0.0°

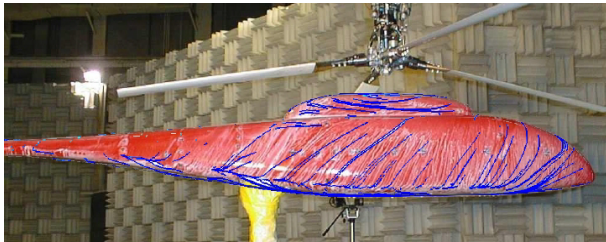
Mineck et al⁽⁷⁾ supplies time averaged data for 12 points measuring transient pressures on the upper surface of the centre line. First comparing the pressures on the centre line shows that the standard $C_T = 0.00636$ case predicts the pressure on the top of the fuselage well; for most of the fuselage length the predictions lie close the experimental values, except for the nose section and behind the cowling (Figure 8).

The pressure distribution for the double thrust case is too high by a factor of two. There are however two sections in which that data predicts the trends well. The first is the nose section; although the pressure is predicted too high, the data predicts the higher pressure ahead of the cowling leading edge, which is not shown in the standard case. This higher pressure corresponds to the leading edge impact point of the rotor wake, which is correctly predicted by the double thrust case, as is also evident from the streak lines.

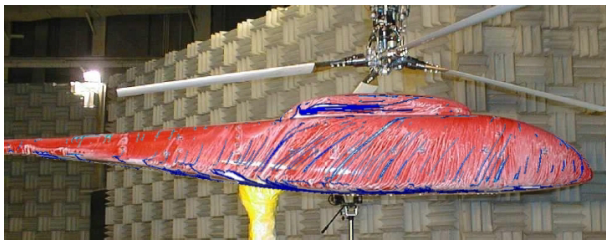
The second area that the double thrust case predicts the trend well is at the trailing edge of the cowling. Though not exactly captured, the low-pressure region is as a result of the rotor hub. For the standard case no evidence of the hub wake is seen.



(a) Original Experiment, form Mineck⁽⁷⁾

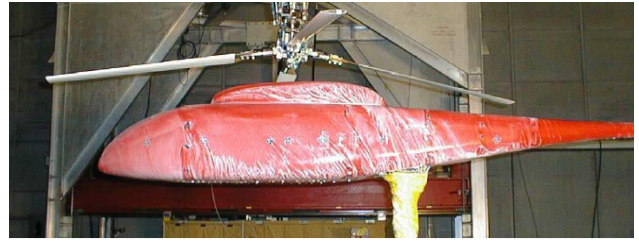


(b) CFD results superimposed, $C_T = 0.00687$

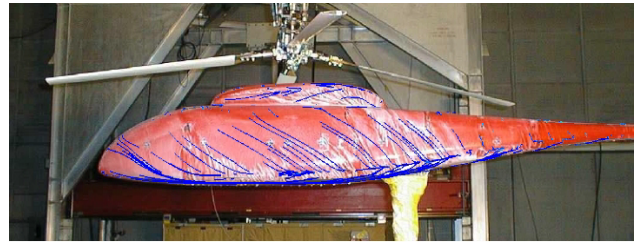


(c) CFD results superimposed, $C_T = 0.0134$

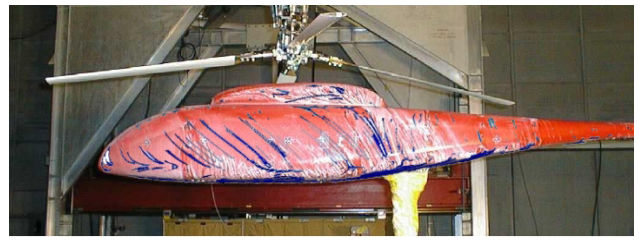
Figure 6 Streak lines, Experimental vs. Numerical on Advancing Side



(a) Original Experiment, form Mineck⁽⁷⁾



(b) CFD results superimposed, $C_T = 0.00687$



(c) CFD results superimposed, $C_T = 0.0134$

Figure 7 Streak lines, Experimental vs. Numerical on Retreating Side

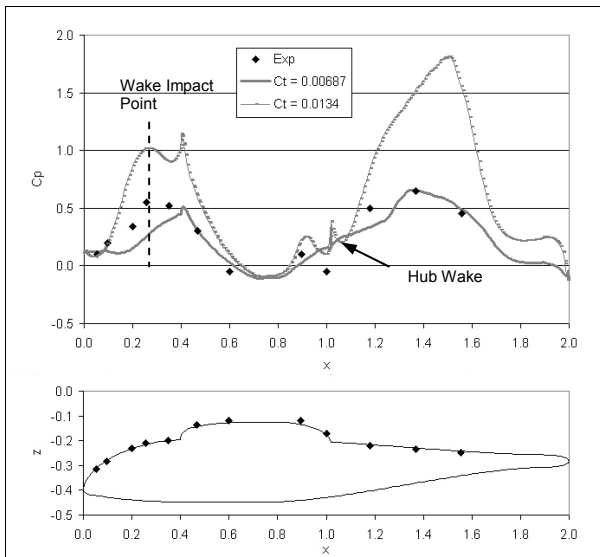


Figure 8 Pressure Distribution on Centre Line, Upper fuselage

Comparing the pressure distributions at the four cross-sectional stations shows that, in general, the better the pressure on top of the fuselage is

predicted (essentially the stagnation point) the better the pressure distribution around the fuselage is predicted. Data from Mineck et al⁽⁷⁾ is represented by "Exp 1" in the figures while data from Freeman et al⁽⁸⁾ is represented by "Exp 2".

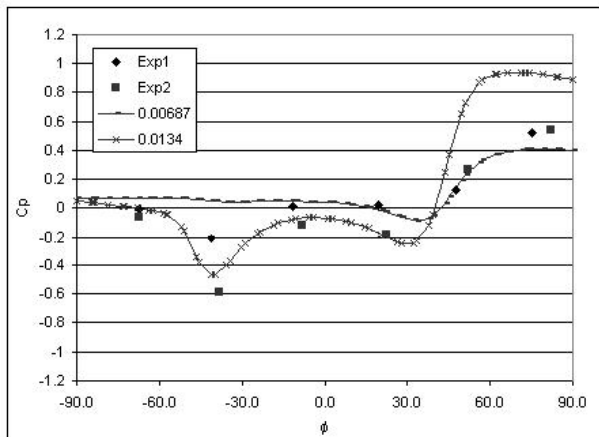
For the station at $x = 0.350R$ (Figure 9) none of the two cases predicts the pressure distribution around the fuselage correctly, though the double thrust case again captures the trend better by displaying the low-pressure at the $\phi = -40^\circ$ position on the advancing side. This is as a result of the rotor wake passing that position which does not occur in the standard thrust case. The pressure contour on the upper half ($0^\circ < \phi < 90^\circ$ on advancing, $-90^\circ < \phi < 0^\circ$ on retreating side) on both sides is however sufficiently well predicted by the standard case. On the plot for the retreating side the predictions of Chaffin et al⁽⁸⁾ (C&B on the legend) are plotted as well. Their predictions show a pressure trough at the $\phi = 40^\circ$ position in Figure 9 (b) which is not evident in the experiments. This is attributed to a lack of prediction of the separation point on the lower corner of the fuselage in their simulations. Thus the current

simulations are a small improvement of what has been achieved till now.

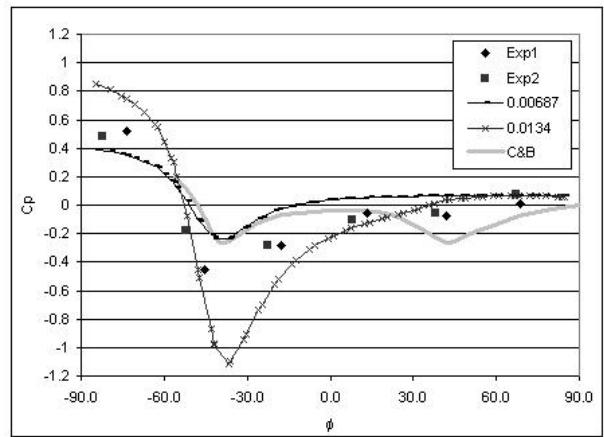
At the section $x = 1.170R$ (Figure 10) the double thrust case predicts the stagnation pressure well, and following on this the general pressure distribution is well presented. The low-pressure spike, (which is especially well presented by the Freeman⁽⁹⁾ data, $\phi = 40^\circ$ on the advancing side) is a result of the hub-wake influencing that point. The shallower angle the hub-wake forms for the standard case means that the wake does not have such a strong influence, as seen by the CFD data. The low-pressure trough on the upper surface

($\phi = -40^\circ$) on the retreating side is however not captured by any of the two cases. None of the troughs on the retreating side are captured by the Chaffin et al⁽¹⁰⁾ results. To note here is also the differences in the two experimental data sets.

For the last two sections at $x = 1.350R$ and $x = 1.540R$ (Figure 11 and Figure 12) both cases give reasonable answers, though the standard case on average gives more accurate results, especially, as already discussed, the pressure on the upper surface of the fuselage. Whereas the double thrust case over predicts the pressures, but clearly follows the trends.

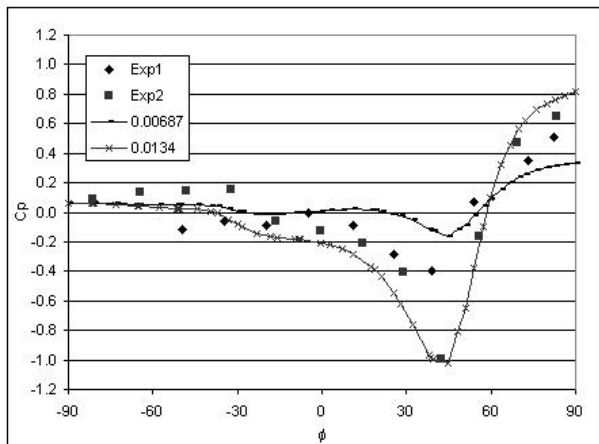


(a) Advancing

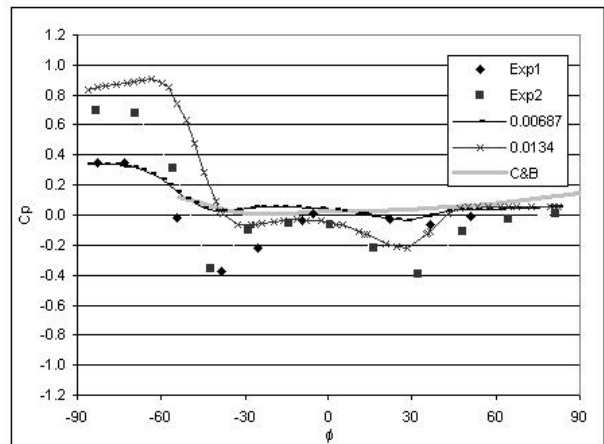


(b) Retreating

Figure 9 $x = 0.350R$

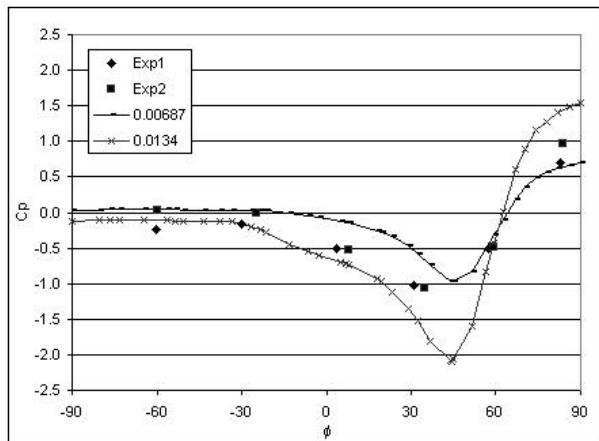


(a) Advancing

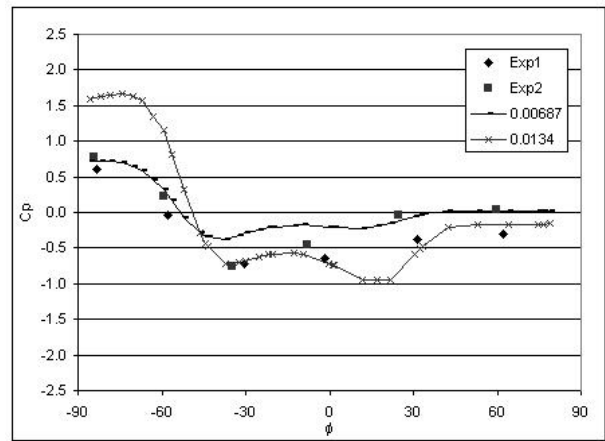


(b) Retreating

Figure 10 $x = 1.170R$

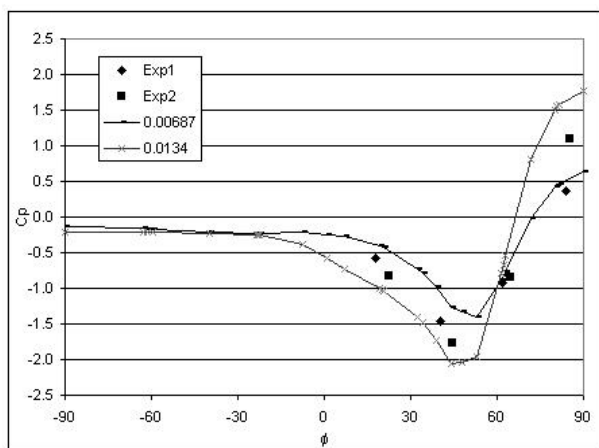


(a) Advancing

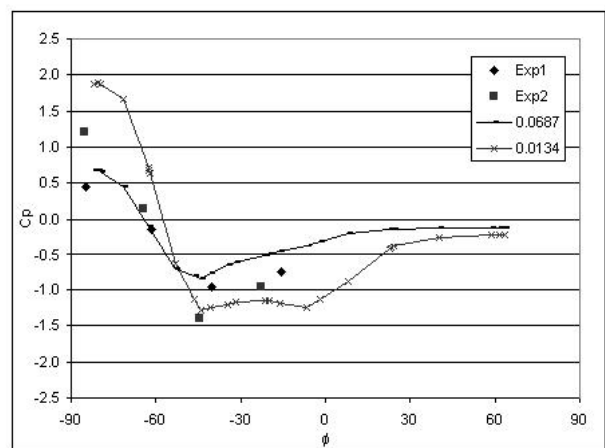


(b) Retreating

Figure 11 $x = 1.350R$



(a) Advancing



(b) Retreating

Figure 12 $x = 1.540$

Conclusion

It would appear from the foregone analysis that a significant contribution to the differences of the numerical data is the angle the rotor wake makes relative to the fuselage. Using the average induced velocity from the CFD results in a basic momentum analysis confirms that the actuator disk does produce the specified thrust. Further comparing the load distribution of the rotor for the two cases shows that the rotor with the high thrust setting has a higher loading at the leading and trailing rim of the rotor; the standard thrust case even has a significant portion of the rotor leading edge experiencing an up-wash through the rotor. This will have a significant effect on the structure downwash; a higher loading at the leading edge forces more air downwards at the leading edge.

Further reasons identified for the difference of the numerical to the experimental downwash distribution is the lack of coning and the tilt of the tip path plane. Both these factors influence the load distribution on the rotor and hence the rotor-wake.

Also, the method of determining the blade section angle of attack can introduce some error at the leading edge of the disk. In the trial done by Hotchkiss⁽⁵⁾ with this method a shrouded fan was modelled. Unlike that fan the current rotor is not shrouded and this allows the flow pattern to change noticeably between the upstream reference disk and the actuator disk itself, especially at the leading edge of the rotor.

As already stated the aim is to develop a method by which rotorcraft intake aerodynamics can be evaluated, and the hub with its control rods can have significant effects on the local aerodynamics around the intakes. All the simulations here were done on a PC desktop machine. The computational effort is low and thus the method forms a useful evaluation tool. Useable results have been obtained from these simulations, with the actuator disk showing promising results that can be improved with fine-tuning on the basis of the points discussed above. In general the wake angle and downwash have to be predicted correctly for the pressure distribution around the fuselage to be correct. Shown here is that the

pressure distribution on the upper fuselage surface is correctly predicted apart from the leading edge and the trends of the pressure distribution around the fuselage are captured if the wake angle is closer to the experimental.

References

1. Chaffin, M.S., Berry, J.D., (1997), *Helicopter Fuselage Aerodynamics Under a Rotor by Navier-Stokes Simulation*, Journal of the AHS, July 1997, v.42, no.3, pp 235-242
2. Lee, J-K, Kwon, O. J., (2002), *Predicting Aerodynamic Rotor-Fuselage Interactions by Using Unstructured Meshes*, Trans. Japan Soc. Aero Space Science, Vol. 44, no. 146, pp 208-216
3. Thiant, G.D., von Backström, T.W., (1993), *Numerical simulation of the Flow Field Near an Axial Flow Fan Operating Under Distorted Inflow Conditions*, Journal of Wind Engineering and Industrial Aerodynamics
4. Meyer, C.J., Kröger, D.G., (2002), *Numerical Simulation of the Flow Field in the Vicinity of an Axial Flow Fan*, International Journal of Numerical Methods in Fluids
5. Hotchkiss, P.J., (2004), *Development of a rotor model for the numerical simulation of helicopter exterior flow-fields*. M.Eng thesis, University of Cape Town,
6. Fluent News, (2005) Vol. XIV Issue 1, pp34-35
7. Mineck, R.E., Althoff Gorton, S., (2000), *Steady and Periodic Pressure Measurements on a Generic Helicopter Fuselage Model in the Presence of a Rotor*, NASA TM 2000-210286
9. Freeman, C.E., Mineck, R.E., (1979), *Fuselage Surface Pressure Measurements of a Helicopter Wind-Tunnel Model with a 3.15 Meter Diameter single Rotor*. NASA TM 80051
10. Chaffin, M.S., Berry, J.D., (1995), *Navier-Stokes Simulation of a Rotor Using a Distributed Pressure Disk Method*, 51st Annual Forum Proceedings, American Helicopter Soc. May 1995, pp 112-136